CR-172107

CSDL-P-2827

FREQUENCY BASED LOCALIZATION OF STRUCTURAL DISCREPANCIES

by

G. D. Shepard*
J. Milani

October 1988

Department of Mechanical Engineering,
Modal Analysis and Control Laboratory,
University of Lowell, Lowell MA., 01854 USA;
*(also Charles Stark Draper Laboratory, Inc.,
Cambridge, MA 02139 USA)

(NASA-CR-172107) FREQUENCY BASED LOCALIZATION OF STRUCTURAL DISCREPANCIES (Draper (Charles Stark) Lab.) 25 p CSCL 20K

N89-13809

Unclas

G3/39 0177608

The Charles Stark Draper Laboratory, Inc.
555 Technology Square
Cambridge, Massachusetts 02139

FREQUENCY BASED LOCALIZATION OF STRUCTURAL DISCREPANCIES

G. D. Shepard† and J. Milani

Department of Mechanical Engineering, Modal Analysis and Control Laboratory, University of Lowell, Lowell MA., 01854 USA; †(also Charles Stark Draper Laboratory Inc., Cambridge, MA. 02139 USA)

ABSTRACT

The intent of modal analysis is to develop a reliable model of a structure by working with the analytical and experimental modal properties of frequency, damping and mode shape. In addition to identifying these modal properties it would be desirable to determine spatially which parts of the structure are modelled poorly or well. This information could be used to improve the finite element model, or to point to faults in the structure and hence help to evaluate mechanical integrity.

This paper shows how the pattern of discrepancies in the analytical and experimental test values for the pole and the driving point zero frequencies of a structure can be linked to discrepancies in the mass or stiffness of the structural elements. This localization technique requires only that mode frequency discrepancy data be measured. The more difficult to obtain mode shape data does not have to be measured, since it is adequate to use the less accurate mode shape data from a finite element model.

The success of this procedure depends on the numerical conditioning of a modal reference matrix. Strategies to insure adequate numerical conditioning require a formulation which avoids geometric and energy storage symmetries of the structure, and ignores structural elements which contribute negligibly small potential or kinetic energy to the excited modes. Physical insight into the numerical conditioning problem is provided by a numerical example and by the localization of a mass discrepancy in a real structure based on laboratory tests.

1. INTRODUCTION

Obtaining a reliable dynamic model for a structure using the technique of modal analysis [1] involves the measurement of the modal parameters of mode shape and frequency, and the linking of these parameters to the modal data of an analytical model. While it is useful to refine the modal model by this technique, the answers to many important structural questions lie in the physical rather than the modal domain.

Modal model refinement involves working with the discrepancies between experimental modal data and the corresponding data from the analytical model. The technique of localization makes it possible to link discrepancies in the frequencies and mode shapes of a structure to discrepancies in the mass or stiffness parameters of the structure. Starting with a pattern of discrepancies in frequency and mode shape in the modal domain, it is possible to locate spatially, in the physical domain, which structural elements have been modelled poorly or well.

It is also possible, by forming a frequency discrepancy vector which compares experimental frequencies measured at two separate times, to determine which structural elements may have been damaged in that interval. Beyond being useful for model verification, localization can improve the accuracy of answers to such physical domain questions as stress, fatigue, operational red lines, and mechanical integrity evaluation.

Localization techniques typically require experimental and analytical information on both frequency and mode shape discrepancies. [2, 3] An earlier paper [4] has shown that it is sufficient to rely on the analytical mode shape data from a finite element program, even if such data lacks accuracy, since first order errors in mode shape cause only second order errors in the localization procedure. It is only necessary to measure the frequency discrepancies, a greatly simplified task, with important practical benefits when the testing has to be done in a difficult environment such as on-orbit. In [4] this frequency discrepancy based localization procedure has been demonstrated analytically for a simple four element beam. This report looks more critically at this localization technique, and develops a strategy which assures success with more complicated structures.

Experience with frequency discrepancy based localization has shown that it is necessary, in a practical application, to control errors in the finite element analysis and in the experimental data, and to deal with the problem of numerical conditioning. This report focuses primarily with the strategy for dealing with numerical conditioning. In addition, examples of the former two error sources, the analytical and experimental, are included, based on some experiments with a real structure that were conducted at the University of Lowell [5].

2. FREQUENCY BASED LOCALIZATION PROCEDURE

We review briefly the frequency based localization procedure. More details are given in Ref [4]. The link between frequency discrepancies and structural element discrepancies is based on an energy method which starts with the Rayleigh Quotient for a particular mode:

$$\omega^2 = V/T \qquad (1)$$

where $V = \Sigma\, v_j$ is the sum of the potential energies of the mode stored in the elements of the structure, and

$\omega^2\, T = \omega^2\, \Sigma\, t_j$ is the sum of element kinetic energies of the mode

Next, cast this equation in differential form using logarithmic differentiation:

$$2\, d\omega/\omega = (dv_1/V\text{-}dt_1/T) + (dv_2/V\text{-}dt_2/T) + (dv_3/V\text{-} \ldots \qquad (2)$$

The quantities ω, V, and T for the mode can be determined from the analytical model, henceforth assumed to be a finite element model. The frequency differential $d\omega$ is equal to the small difference between the finite element frequency and the experimental frequency of the particular mode in question, or the small difference between two experimental values taken at two different times. By suitable approximations [4], the equation can be cast in the form:

$$2\, d\omega/\omega = [\,(v_1/V)(dk_1/k_1)\text{-}(t_1/T)(dm_1/m_1)] + [\,(v_2/V)(dk_2/k_2)\text{-} \,.. \qquad (3)$$

where k_j is a stiffness scale factor (modulus), and m_j is a mass scale factor associated with element j.

Equation (3) is a linear equation which relates the mode frequency discrepancy ratio $d\omega/\omega$ to the stiffness and mass discrepancy ratios for each of the elements. The weighting factors v_j/V and t_j/T for each element are based on the mode shapes from the finite element analysis. More equations of the form of equation (3) can be generated by considering additional modes, either pole modes or driving point zero modes. When assembled into matrix form, the equations take the form of equation (4). The coefficients of, say, p equations, form a (p x n) modal reference matrix which relates the (n x 1) structural discrepancy vector to the (p x 1) frequency discrepancy vector. Solving for the dependent structural discrepancy vector proceeds directly, provided the modal reference matrix is well conditioned. If $p > n$, the solution involves the use of the pseudo inverse of the modal reference matrix.

$$
\begin{bmatrix}
\frac{v_1^{(1)}}{V} & \frac{v_2^{(1)}}{V} & \cdots\cdots & \frac{t_k^{(1)}}{T} & \cdots \\
\frac{v_1^{(2)}}{V} & \frac{v_2^{(2)}}{V} & \cdots\cdots & \frac{t_k^{(2)}}{T} & \cdots \\
\cdots & \cdot & \cdot & \cdots & \cdot \\
\cdots & \cdot & \cdot & \cdots & \cdot \\
\frac{v_1^{(p)}}{V} & \frac{v_2^{(p)}}{V} & \cdots\cdots & \frac{t_k^{(p)}}{T} & \cdots
\end{bmatrix}
\begin{bmatrix}
\frac{dk_1}{k_1} \\ \frac{dk_2}{k_2} \\ \vdots \\ \frac{dm_k}{m_k} \\ \vdots
\end{bmatrix}
=
\begin{bmatrix}
\frac{d\omega^{(1)}}{\omega} \\ \frac{d\omega^{(2)}}{\omega} \\ \vdots \\ \frac{d\omega^{(p)}}{\omega}
\end{bmatrix}
\qquad (4)
$$

3. NUMERICAL CONDITIONING OF THE MODAL REFERENCE MATRIX

Success with the localization procedure depends on the numerical conditioning of the modal reference matrix. A standard indicator of the numerical conditioning of a matrix is the condition number, C_n, [6] which is the ratio of the highest to the lowest eigenvalue of the matrix. This number varies over the range $1 \leq C_n \leq \infty$, the larger the value the poorer the numerical conditioning. In developing a strategy for frequency discrepancy based localization, the condition number is of limited use because it only serves to confirm what is already known. To see this, we point out first that the elements of the modal reference matrix are determined by the choice of the structural elements whose discrepancies are of interest. Some structural element choices lead to poor localization results, and have large condition numbers, while other element choices lead to good localization results, and have lower condition numbers. The monitoring of the condition number serves only to confirm that numerical conditioning is of crucial importance to localization. The condition number itself gives no insight into the question of which structural elements will be good choices.

Two criteria have been adopted which provide a strategy for selecting good structural elements for the localization procedure. Mathematically, both criteria have to do with the column space of the modal reference matrix. These criteria will be described separately below, along with the physical insights which complement the mathematical reasoning behind the criteria.

3.1 CRITERION 1: COLUMN VECTOR ORTHOGONALITY

Putting aside the condition number as a constructive indicator of good choices for structural discrepancies, we turn to the column space vectors of the modal reference matrix. For equation (4) to be solved successfully it is necessary that these vectors be independent, that is, that no two (or more) vectors be parallel to each other. The numerical conditioning of the modal reference matrix deteriorates as the vectors become closer to being parallel. Thus, the strategy for good numerical conditioning reduces to a search for a set of column vectors which are as orthogonal to each other as possible.

From a physical viewpoint, an important cause for two column vectors of the modal reference matrix to be nearly parallel is symmetry - both geometric and energy storage symmetry. A simple example of geometric symmetry is a free-free uniform beam. The column vector which represents the pattern of pole frequency changes caused by a mass change at the left hand beam tip will be identical to the vector which represents pole frequency changes which correspond to mass changes at the right hand beam tip.

The free-free beam also provides an example of energy storage symmetry. The pattern of pole frequency changes caused by a change in stiffness at, say, the center element, is nearly the same, except for a negative sign, as the frequency change pattern caused by a mass change to the same element. In this case, computations have shown that the energy storage symmetry is strong, the vectors are nearly parallel, and the modal matrix is nearly singular. A second energy storage symmetry example is not so obvious: direct calculation has shown that the pattern of pole frequency changes caused by a stiffness change to the root of a cantilever beam is identical, except for a negative sign, to the pattern of pole frequency changes induced by a mass change at the tip of the cantilever.

Symmetry, then, of both geometric and energy storage kinds, gives rise to poor numerical conditioning, and success with localization requires that the amount of symmetry be limited Fortunately, the above examples, while they lend themselves to simple intuitive insights into the effects of symmetry on numerical conditioning, are not likely to be met in practice. Real engineering structures typically lack such strong symmetry, and the modal reference matrix is correspondingly less likely to suffer from poor numerical conditioning.

The inclusion of zero frequencies along with the pole frequencies reduces the level of symmetry. The mode shape which corresponds to a driving point zero is identical to the pole mode shape of the structure with a new boundary condition where the driving point is fixed. The symmetry of even a symmetrical structure is thereby reduced by the unsymmetric boundary condition. Further, whatever symmetry exists with the added zero mode boundary condition is different from the symmetry imposed by the original pole mode boundary conditions. When both dissimiliar symmetries of the pole and the zero modes are combined in the modal reference matrix data base, the overall symmetry of the formulation is reduced.

3.2 NUMERICAL EXAMPLE: TIP EXCITED ASYMMETRIC BEAM

We pass now to a specific numerical example to help set the general ideas discussed above. Consider the structure in Fig. 1(a): a free-free beam of 15 macro elements driven by a force at the right hand end. The perfect mass symmetry of the beam has been reduced by a concentration of mass at macro elements 5 and 6. The structural discrepancy coordinates for equation (4) are shown in Fig. 1(b): 1-15 for the dk/k 's, and 16-30 for the dm/m 's.

(Figure 1(a) about here)

(Figure 1(b) about here)

Indicated also in this figure is the fact that the elements of the modal reference matrix are computed from a more detailed finite element model which has 5 micro elements for every macro element.

The symmetry of the structure, and, therefore, the numerical conditioning of the formulation, is most easily understood by studying the orthogonality matrix for the column vectors of the modal reference matrix, shown in Fig. 2. Each element in this matrix represents the square of the normalized dot product of two vectors in the modal reference matrix. Such a matrix is symmetric about its main diagonal so only the upper triangular matrix is shown. Two vectors are parallel when their squared normalized dot product is unity. They are orthogonal when this product is zero. To focus attention on vectors which are weakly orthogonal, only products which are ≥ 0.6 are shown.

(Figure 2 about here)

A key to the orthogonality matrix which identifies the various types of symmetry in this particular example is shown in Fig. 3. Elements of the orthogonality matrix which are near unity correspond to column vectors in the modal reference matrix which are nearly parallel. For this example these nearly parallel vectors can be explained by the geometric or the energy storage symmetries which show up as bands in Fig. 3.

(Figutre 3 about here)

This beam example, even with the addition of some concentrated mass at macro elements 5 and 6, still shows considerable symmetry. The stiffness symmetry, represented by the near unity elements in the k geometric symmetry band of the kk sub matrix, is quite strong even though the driving point zero frequencies have been included in the formulation (Had they not, the k geometric symmetry band would have been unity.). The mass symmetry, judged by the sparse and smaller sized entries in the m geometric band of the mm sub matrix, is less severe. The numerical conditioning of the modal reference matrix based on the dm/m discrepancies of all the 15 macro elements of the beam is fairly good (condition number Cn = 39), good enough for a numerically simulated mass change of 20% to element 1 to be easily discerned (Note that this 20% change to a single macro element represents a change of only 1.3% to the mass of the beam as a whole.). The results of this computation, using the patterns of frequency change of the first eight poles and the first seven zeros, are shown in Fig. 4.

(Figure 4 about here)

3.3 CRITERION 2: COLUMN SUMS

The second strategy for selecting structural elements makes use of what is called "column sums". A column vector of the modal reference matrix indicates the percent changes in pole or zero frequencies that result from changing a particular dk/k or dm/m of the structure. If the column sum, that is, the sum of the magnitudes of the elements of a particular column vector, is small compared with the column sums of other vectors, then changes affecting the mass or stiffness of the particular structural element will have a comparatively small effect on frequency changes. For instance, the column sum of the vector which represents the effect of stiffness changes to the tip element of a cantilever beam will be small compared to the column sum which corresponds to a stiffness change of the root element.

Whether the column sum corresponding to a particular structural element is small or not depends on the bandwidth of the pole or zero frequencies chosen for the localization procedure. If new pole or zero frequencies are introduced, the significance of a column sum may change. For the example of the cantilever beam, the column sum which corresponds to the tip element will grow larger as the bandwidth of the poles and zeros increases, since at high frequencies even the tip of the beam begins to flex. It makes sense, then, to choose candidate poles and zeros from the bandwidth that will receive excitation in an actual situation.

A structural element which has a negligibly small column sum need not be assessed at all because that element will not be significantly excited in practice. From a numerical viewpoint it is probably not wise to include an element with a negligible column sum because the resulting structural discrepancy estimate is likely to be contaminated by noise. Conversely, if it is deemed important to assess a particular structural element, then the structure must be excited over an adequate bandwidth so that substantial potential energy (for a stiffness discrepancy assessment) or kinetic energy (for a mass discrepancy assessment) is generated in the structure.

The column sums for the 15 element free-free beam example are shown in Fig 5. The column sum of 0.18 associated with the first column of the modal reference matrix - that is, the vector which gives the pattern of frequency changes caused by changes in the dk/k stiffness ratio of the left hand tip of the beam - is small compared to all the other column sums. It is therefore not advisable to include the dk/k of the left hand tip of the beam

(Figure 5 about here)

as one of the dependent variables. Note that the column sum of 0.37 at the right hand end of the beam is not as negligible as the left hand value. This is because the driving point, and therefore the driving point zeros, are at the right hand end of the beam. The structure near the node at the right hand end is more heavily flexed, and stiffness changes to macro element 15 affect the zero frequencies more than stiffness changes to macro element 1 at the left hand end of the beam, where the beam flexes little.

3.4 EXPERIMENTAL EXAMPLE: TIP LOADED SYMMETRIC BEAM

Tests on a uniform, symmetrical free-free beam were made at the University of Lowell. [5] This beam and the test set up were identical to that shown in Figs. 1(a) and 1(b) except that the asymmetrical mass was not added to macro elements 5 and 6. In one experiment both pole and driving point zero frequencies were measured on the uniform beam. The beam was then modified by physically adding a 20% mass change to macro element 1 (left hand tip of the beam). Again the new pole and zero frequencies were measured. The frequency discrepancies determined by these two tests are shown in Fig. 6.

(Figure 6 about here)

To apply the localization procedure a frequency discrepancy vector was formed from the measured pole and zero discrepancies shown in Fig. 6. Because the beam was so symmetrical it was difficult to choose suitable discrepancy elements on the beam that provided an adequately independent set of column vectors for the modal reference matrix. One nearly successful set of beam discrepancy elements consisted of dk/k coordinates 2,3,5,7,9, and dm/m coordinates 16, 19, 21, 23, 25, 26, 27, 28, and 30. Note that because of the strong symmetry of the uniform beam it was not possible to include discrepancies for all 15 macro elements (discrepancy of macro element 14 is missing)

The frequency discrepancy localization procedure was applied to this measured discrepancy vector, with the results shown in Fig. 7. The success of this localization shows two important results: first, that it is possible to keep the experimental error low enough for the procedure to work, even though the numerical conditioning is rather poor (Cn = 122), and second, that it is possible to find a set of sufficiently independent column vectors for the modal reference matrix, even though the beam has very strong symmetry. As mentioned above, this second result is made possible only because driving point zeros were included in the localization procedure.

(Figure 7 about here)

In contrast, the same localization of the beam was attempted using an estimated frequency discrepancy vector based on the uniform, unflawed beam poles and zeros obtained from the finite element model. The estimated frequency discrepancies are shown in Fig. 8. When

(Figures 8 and 9 about here)

compared with the measured frequency discrepancies (Fig. 6), these estimated frequency discrepancies show some systematic error. The resulting localization (Fig. 9), for the same choice of macro element discrepancies as before, is unsuccessful. Note that the dm/m discrepancy for the flawed macro element mass is large and has the wrong sign, also the large number of spurious discrepancies at the other unflawed elements.

The breakdown of the localization procedure reveals that the procedure is sensitive to errors in the frequency discrepancy vector - in this case the noise introduced by the fact that the finite element model did not predict frequencies close enough to the real test data. For this example, the sensitivity is extreme: finite element modelling errors of the order of 1% cause the localization to break down. The important point is that this extreme sensitivity has to do with the poor numerical conditioning.

Both examples (Figs. 7,9) have the same marginal numerical conditioning (same C_n = 122). The localization of Fig. 7 is successful in spite of the poor conditioning because the input vector error is so small. This is not so for the localization shown in Fig. 9 where the substantial error introduced by the noisy input vector is amplified by the poor numerical conditioning. The localization shown in Fig. 9 can be improved by improving the numerical conditioning. Removing discrepancy coordinate 2 (dk/k of macro element 2) from the formulation, reduces the C_n from 122 to only 22. The resulting localization, shown in Fig.10, is notably improved even though the error in the input vector still exists.

(Figure 10 about here)

The localization of Fig. 10 deserves further comment. First, the 20% mass flaw at macro element 1 , which physically exists on the test beam, has been localized successfully both in sign and in magnitude. The next highest discrepancy, a +15% discrepancy in the mass of macro element 15, must be attributed to an error in the finite element model. This is a plausible modelling error: although the finite element model of this test beam properly accounted for the translational mass of the accelerometer and the load cell at the right hand end of the beam (Fig. 1), it neglected to include the rotational inertia of these two transducers. So although the input vector contains significant error, the dominant results of the localization still yield useful information on structural changes and finite element modelling errors .

In summary, there are three aspects of the localization procedure which are necessary for success:

- structural element discrepancies which actually exist, either physically or analytically, must be provided for in the formulation, i.e. included in the output (structure element discrepancy) vector.
- input (frequency discrepancy) vector noise must be kept low
- output vector elements must be chosen insure good numerical conditioning

4. APPLICATIONS

The success of the frequency based localization procedure described above suggests two applications: (a) structural integrity monitoring, and (b) misassembly detection.

Structural integrity monitoring. Starting with a modal reference matrix which is based on a finite element model, a baseline measurement of pole and driving point zero frequencies of the real structure is made. Next, a subsequent structural integrity monitoring test is made, and a frequency discrepancy vector formed. Finally, a localization is performed to see if there are any structural changes.

For structural integrity monitoring it may be acceptable to assume that mass discrepancies are zero and that it is only necessary to monitor dk/k changes which would result from structural flaws. By ruling out dm/m changes the number of frequencies to be measured is reduced by a factor of two.

Misassembly detection. This application of localization follows the structural integrity monitoring procedure, but with one significant difference. The baseline frequency measurements are replaced by estimates from a realistic finite element model.

5. CONCLUSION

The results of this study indicate that the first application of localization, structural integrity monitoring, is practical and feasible at its present level of development. Frequency based localization is particularly well suited for on-orbit applications where mode shape information is more difficult to obtain than in an earth laboratory. The present work suggests that the second application of localization, misassembly detection, is promising, but that it places high demands on the accuracy of the finite element model.

ACKNOWLEDGEMENTS

This paper was prepared by The Charles Stark Draper Laboratory, Inc., under Contract NAS9-17560 with the National Aeronautics and Space Administration.

REFERENCES

1. D.J. Ewins 1984 *Modal Testing: Theory and Practice*, New York: John Wiley & Sons.
2. O. Zang and G. Lallement 1987 *Mechanical Systems and Signal Processing* 1(2), 141-149, Dominant Error Localization in a Finite Element Model of a Mechanical Structure
3. J.C. O'Callahan and C-M. Chou 1988 *Proceedings of the 6th International Modal Analysis Conference, Orlando, Florida*. Localization of Model Changes for Optimized System Matrices Using Modal Test Data.

4..G.D. Shepard 1987 *Proceedings of the 5th International Modal Analysis Conference, London, England*. Spatial Distribution of Model Error Based onAnalytical/Experimental Frequency Discrepancies.

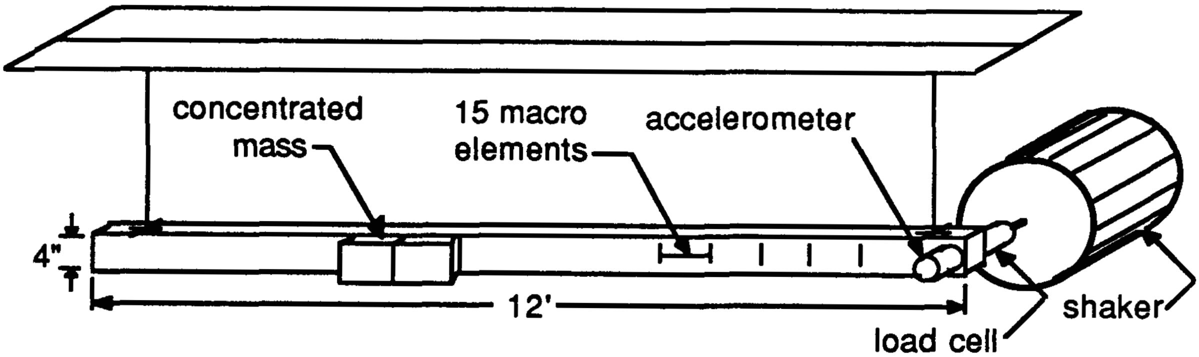

Figure 1(a) Tip Excited Asymmetric Beam

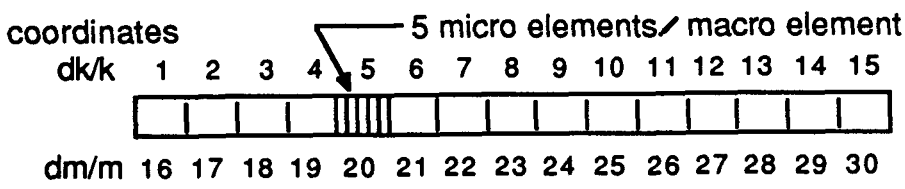

Figure 1(b) Discrepancy Coordinates

1				5					10					15					20					25					30	
1	.82													.68																1
	1												.83	.75		.60	.64	.69	.62		.74							.71		
		1	.61									.77	.66				.89			.61							.71			
			1	.67	.63	.63					.80	.79			.61			.77	.72	.69	.68		.72			.75	.74			
				1	.63	.63				.83	.69				.68	.63			.92	.61	.62		.61		.81	.64		.62		5
					1	.71			.82	.65	.63				.76	.67				.95				.80				.64		
						1	.61	.84	.64	.62					.85	.81				.72	.80		.74							
							1	.63							.63						.62	.89								
								1	.60						.78	.74					.69		.91							
									1	.63	.60				.74	.66				.72				.94						10
										1	.61				.73	.65			.69						.95					
											1	.62			.61				.71	.63			.61	.63		.96				
												1					.60	.61	.61		.63		.66				.95			
													1	.65			.66	.62	.68	.63	.71	.63		.60		.61	.62	.88		
														1														.69		15
															1	.68				.67			.65	.60						
																1				.62	.70		.63							
																	1				.62									
																		1			.70		.62				.60			
																			1		.63		.63		.74	.70		.65		20
																				1			.63	.75		.61		.66		
																					1	.61	.72				.63	.69		
																						1						.61		
																							1				.62			
																								1						25
																									1					
																										1				
																											1			
																												1		
																													1	30

Figure 2. Orthogonality Matrix for Asymmetric Beam

(only elements ≥0.6 are shown)

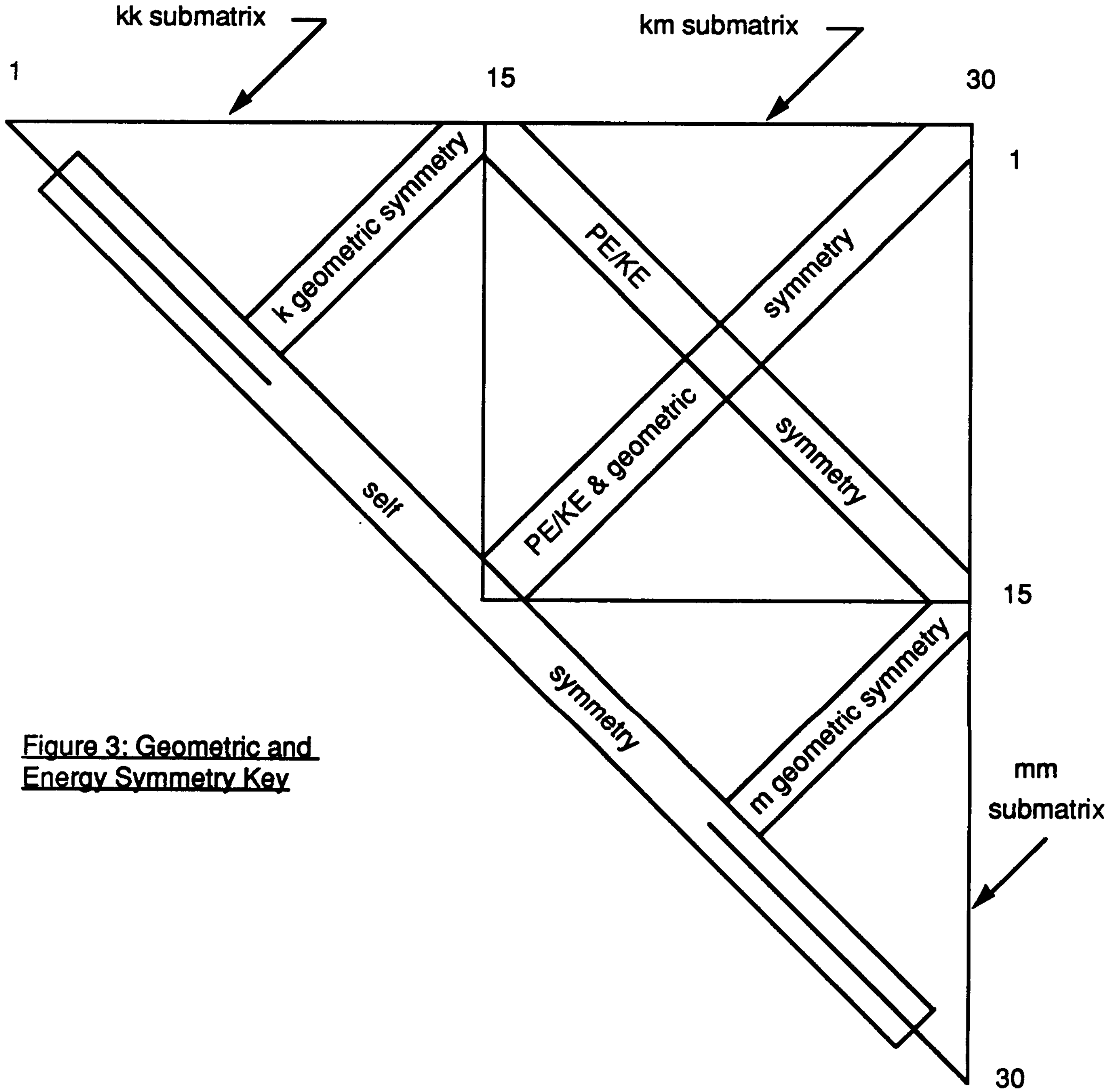

Figure 3: Geometric and Energy Symmetry Key

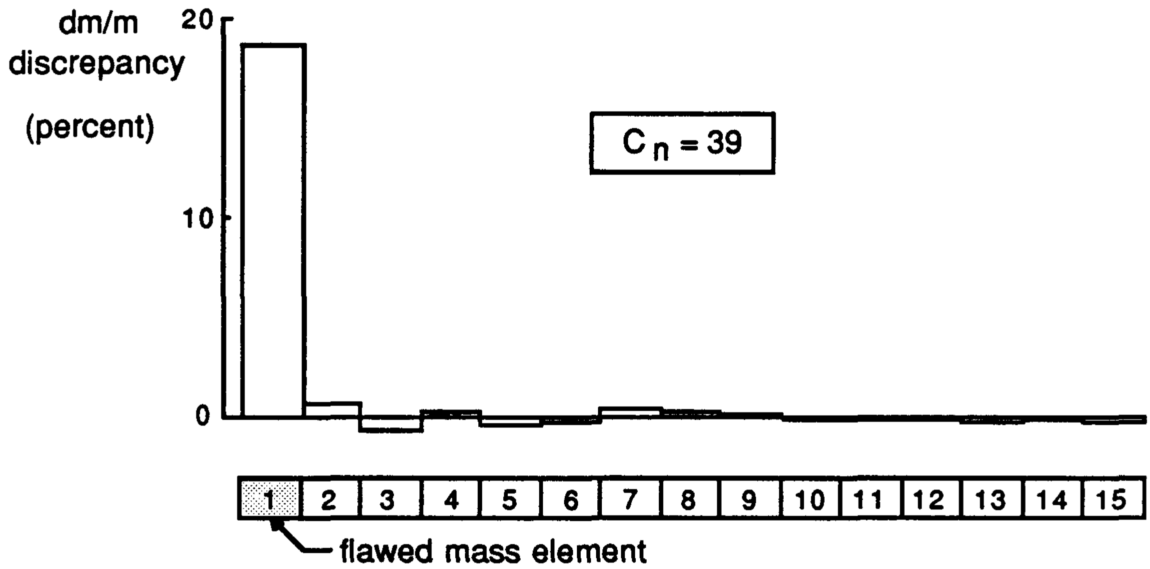

Figure 4. Mass Discrepancy Localization: Asymmetric Beam

	0.18	1.09	1.12	1.23	1.43	1.43	1.21	1.14	1.13	1.14	1.12	1.16	1.09	1.18	0.37
dk/k	1	2	3	4	5	6	7	8	9	10	11	12	13	14	15
dm/m	16	17	18	19	20	21	22	23	24	25	26	27	28	29	30
	1.75	0.95	0.86	0.80	1.27	1.35	0.85	1.03	1.05	1.04	1.01	1.04	0.92	1.04	1.05

(all dm/m 's are negative)

Figure 5. Column Sums: Asymmetric Beam

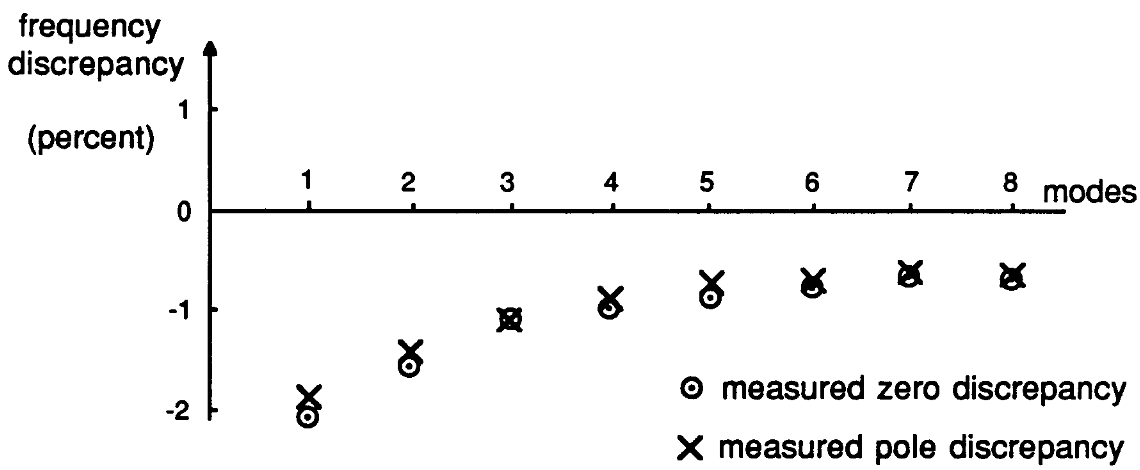

Figure 6: Measured Frequency Discrepancies: Symmetric Beam

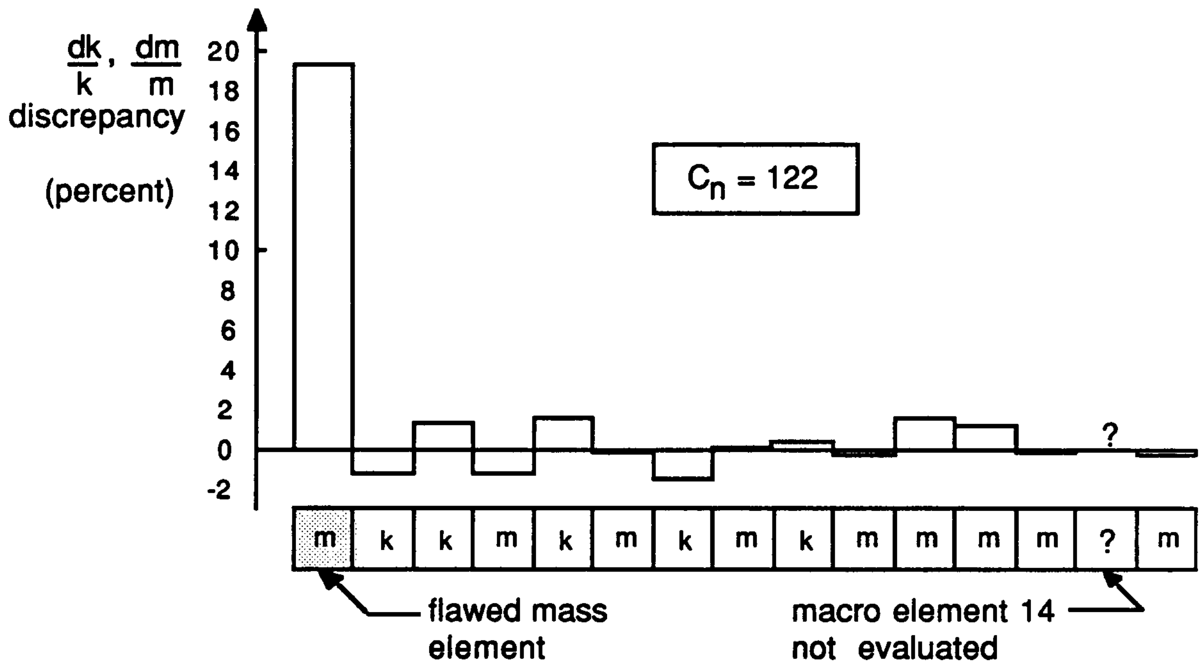

Figure 7: Mass Discrepancy Localization of Symmetric Beam Based on Measured Frequency Discrepancies

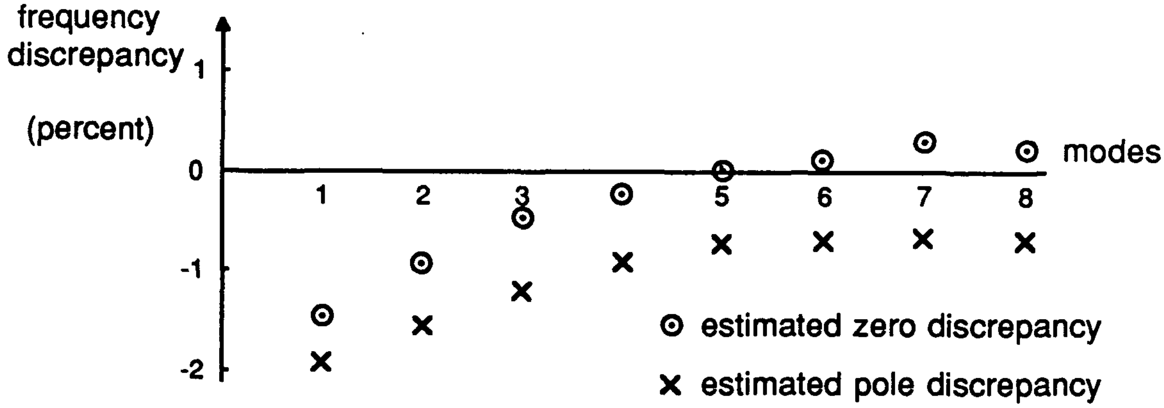

Figure 8: Estimated Frequency Discrepancies: Symmetric Beam

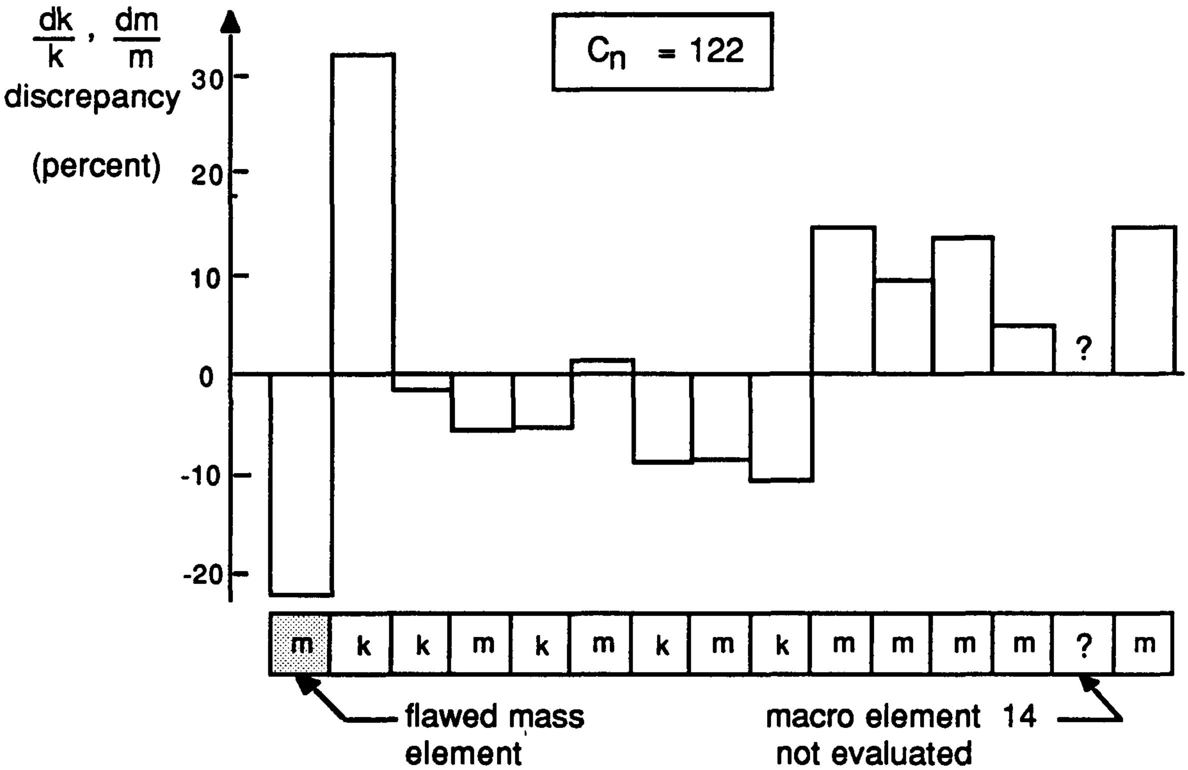

Figure 9: Mass Discrepancy Localization of Symmetric Beam Based on Estimated Frequency Discrepancies

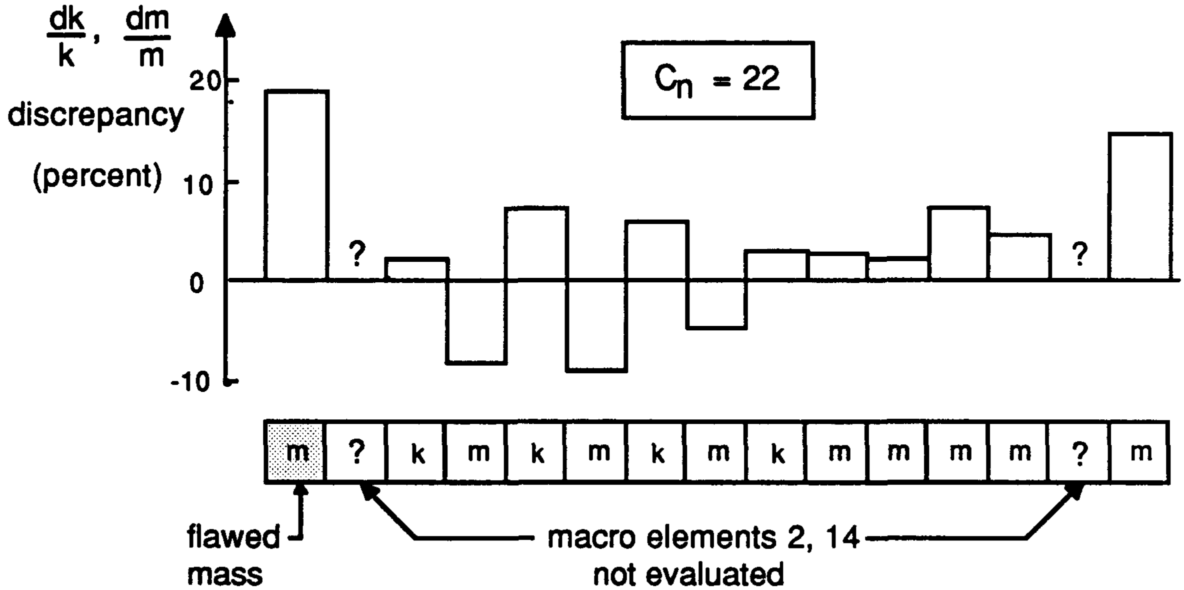

Figure 10: Mass Discrepancy Localization of Symmetric Beam Based on Estimated Frequency Discrepancies